

## **A Study of the Ferrous Oxidation Process in Acidic Mine Seepage**

Jing Y. Liu and Margarete Kalin

Boojum Research Limited, 468 Queen Street E.,

Toronto, Ontario (416) 861 1086. M5A 1T7

### **Abstract**

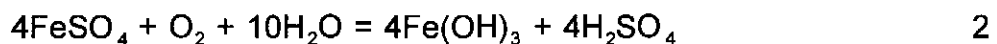
Iron is the dominant element in acid mine drainage (AMD). Its oxidation process is the major factor controlling the pH of AMD. In this work, iron oxidation rates are measured in a field seepage and in several AMD samples in the laboratory. The pH of the AMDs tested ranged from 1.81 to 3.66. Initial ferrous iron concentrations range from 10 mg/L to 4000 mg/L. If other possible microbial and geochemical effects are excluded, then the iron oxidation process in all these examples of AMD can be expressed as a pseudo first order reaction. The rate constants vary from  $0.00017 \text{ min}^{-1}$  to  $0.00030 \text{ min}^{-1}$ . The data are quite consistent with previous studies in buffer systems. The oxidation rate constant can be used to determine retention times for AMD in a field precipitation pond. However, other microbial processes also need to be considered.

### **Keywords**

Acid mine drainage, iron oxidation, kinetics, AMD treatment, precipitation pond

## INTRODUCTION

Acid mine and acid rock drainage (AMD and ARD) are of major environmental concern to the mineral sector worldwide. AMD or ARD originates from the waste rock or tailings, which contain pyrite ( $\text{FeS}_2$ ) or pyrrhotite ( $\text{Fe}_{1-0.8}\text{S}$ ). When these minerals are weathered or change through microbial activity, sulfide is oxidized into sulfate and iron dissolves. As the oxidation proceeds iron is oxidized from ferrous into ferric ions and will further hydrolyse. This process can be simply expressed as -



Reaction 2 is the principal acid-generating step. Since the oxidation state of iron is the major factor controlling the pH of AMD, the rate at which the iron oxidation process takes place is relevant to treatment system design.

When AMD seepages emerge from tailings and waste rock only reaction 1 is completed. At the point of emergence from the tailings dam, the AMD seepages contain ferrous ions, and the pH is frequently neutral to slightly acidic (about 5 to 6). On exposure to the air, ferrous ions are oxidized, to form ferric hydroxide or

goethite ( $\text{FeOOH}$ ) precipitates. These precipitates are also referred to as yellowboy. As oxidation and precipitation proceed, the pH decreases.

The kinetics of the iron oxidation process have been studied extensively under natural conditions and in the laboratory, from both the chemical and biological points of view (Sung and Morgan 1980, Hustwit et al. 1992, Nordstrom 1985, Nakamura et al. 1986, Wichlacz and Olem 1993, Wichlacz and Richard 1993, Okereke and Stevens 1991, Henrot and Weider 1990).

Iron oxidation has been shown to be a reaction related to iron concentration, water pH, and oxygen concentration in water (Sung and Morgan 1980, Hustwit et al. 1992). On the other hand, from a microbiological viewpoint, Okereke and Stevens (1991) found that the iron oxidation rate is significantly assisted by Thiobacillus and is not related to iron concentration.

Consequently, oxidation rates quoted are quite varied. Sung and Morgan (1980) give oxidation rates in the laboratory ranging from  $10^{12}$  to  $10^{14} \text{ M}^{-2}\text{atm}^{-1}\text{min}^{-1}$ . Nordstrom (1985) measured an oxidation rate in a natural AMD stream at about  $10^{20} \text{ M}^{-2}\text{atm}^{-1}\text{min}^{-1}$ . That is six to eight orders of magnitude greater than the laboratory rates of Sung and Morgan, but very similar to values where bacterial

cultures were used in the experiments. Nakamura et al. (1986), using rotating biological contactors, found oxidation rates even higher than Nordstrom's value.

The objective of this work was to address factors controlling iron oxidation rates in different AMD seepage waters, such that the oxidation rate can be used for the design of a natural iron precipitation pond. Field measurements in tailings seepages and laboratory experiments with different AMD seepages are presented.

## **FIELD MEASUREMENT, SAMPLING PROCEDURE, AND ANALYTICAL METHODS**

### Tailings Seepage Characteristics

The field measurements were carried out in a seepage emerging from the Copper Cliff tailings dam (Inco Limited, Canada). The seepage flows year-round at a rate of about 1 L/s. Along the ditch smaller seepages may emerge along the 100 m length of the ditch, depending on hydrologic conditions. The ditch starts as a shallow area about 28 cm wide(W) by 4 cm deep(D) and becomes wider and deeper (70 cm W by 17 cm D) at a distance of about 20 m.

### Field measurement data and calculation procedures

Seven stations along the Copper Cliff tailings seepage were selected: station 1 and station 7 are the closest and the farthest locations, with respect to the origin of the seepage. Stations 3 and 7 are about 11 and 40 m away from station 1. The distance between each station and the average cross-sectional area at each station were also measured. Seepage flow rates at each station were measured with a Montedoro-Whitney PVM-2A flowmeter. The pH and Em (Em is the measured, unconverted Eh value (Hem, 1985)) were measured using a Corning pH 103 meter with an ORP electrode (Fisher 13-620-284) and a calomel reference electrode (Fisher 13-620-52).

Two surface water samples were collected at each station. Plastic sample bottles were filled to the brim, sealed and brought to the laboratory within 24 h for titration and other analysis.

Seepage sample acidometric titrations were performed using a Metrohm 702 SM titrino machine with a combined pH glass electrode. The method adds 0.1 N NaOH incrementally to the AMD, exposed to air. The quantity of titrant and the pH of the AMD are then followed up to a pH of 8.5. This method is a simple, diagnostic tool developed in our laboratory (Liu and Kalin 1991) to semi-quantitatively determine metal concentrations in AMD waters. Several major metal

concentrations and speciation ( $\text{Fe}^{+3}$ ,  $\text{Fe}^{+2}$ ,  $\text{Al}^{+3}$ ,  $\text{Cu}^{+2}$  and  $\text{Zn}^{+2}$ ) can be estimated by the shape of the titration curve.

As the titration proceeds the pH increases, and various metal ions precipitate as their hydroxides. When metal precipitates, solution pH increase slows and plateaus form in the titration curve. Ferric hydroxide has a much lower solubility product than ferrous hydroxide, therefore ferric ions precipitate much earlier than ferrous ions. The former usually precipitate at  $\text{pH} < 3.5$ , while the latter usually precipitate at pH within around 5.5 to 6.5. The pH calculated by  $\text{Fe}(\text{OH})_2$  solubility product is around pH 8. However, in the practical titration process, as water pH approaches 5, ferrous carbonate may form, accelerating ferrous oxidation, forcing precipitation in a much lower pH range. We have titrated more than 25 types of seepages from a number of mines across seven provinces (including the seepage described below). In all these seepages precipitates of ferrous ions are in the range below pH 7.

Ferrous and total iron were measured in each sample separately. Total iron was measured by Hach test FerroVer method. Ferrous was measured by the phenanthroline method (American Public Health Association 1989 #3-105). Other elements as noted were measured by ICP (Inductively Coupled Plasma Spectroscopy) at a certified laboratory.

## LABORATORY EXPERIMENTAL PROCEDURES

Seepage and tailings pore water representing a large range of total iron concentrations were collected for the determination of laboratory iron oxidation rates. The sample locations and the dates of collection are summarized in Table 1. Seepage from a base metal tailings dam was collected from the same location, one sample being aged at room temperature for 1 month (No.1) and another sample for 14 months (No.2).

Two hundred and fifty milliliters of each water sample were placed in graduated beakers of the same shape, and the samples were left exposed to the air, without stirring. Water depth in the beakers was 5 cm. Laboratory temperature was 25° C. The pH, Em, ferrous and total iron were measured frequently. The experiment was terminated after 454 h.

## **RESULTS AND DISCUSSION**

Copper Cliff seepage ditch data are shown in Table 2. The water temperature was 21° C in the entire seepage. Retention time of seepage in the ditch from station to station is calculated by the average volume (average cross

area \* length) divided by the flow rate. Retention time at station 1 is assumed as zero.

To confirm that iron oxidation occurred in the 40 m seepage ditch, titration curves of either one of the two samples from stations 1, 3 and 7 are compared in Figure 1. The titration curve of station 1 starts at the highest pH and has a long flat plateau in the pH range from 6.5 to 7, indicating the presence of ferrous ions. Titration curves of stations 3 and 7 water start at a lower pH, and the plateaus are shorter. This shows that, as the seepage flowed further, ferrous concentration decreased, and water pH dropped. This phenomenon is quite consistent with the chemical reaction equation 2. It suggests that ferrous ions have been oxidized.

In calculating the iron oxidation rate, we met with the difficulty that the total iron concentrations of the seven stations were different, and  $[\text{Fe}^{+2}]$  at latter stations were sometimes higher than  $[\text{Fe}^{+2}]$  at earlier stations. This have been caused by localized wind mixing or smaller seepages may have entered the bulk flow further down stream. However, the average ratio of  $[\text{Fe}^{+3}]/[\text{Fe}^{+2}]$  increased, and Em values generally increased throughout the ditch (see Table 2).

Table 3 details the key elements in the seepage water, as measured by ICP. Elemental concentrations less than 1 mg/L are not listed in the table. The



table indicates that manganese concentration is much lower than iron. Also, sulfur, at the pH and Em of the seepage water, can only be  $\text{SO}_4^{-2}$  ions. From the titration curves and Table 3 we may assume that the Em value changes at each station are mainly related to iron oxidation states.

With these assumptions, the iron oxidation rate can be calculated as follows. From ferrous and total iron concentrations in each sample,  $[\text{Fe}^{+3}]/[\text{Fe}^{+2}]$  ratios are obtained. The log values of the ratios are plotted against Em in Figure 2. A linear relationship between Em and the measured ratio is evident, with the exception of the results from stations 3 and 6. From these measurements, a linear regression line can be fitted ( $r = 0.86$ ), and an empirical equation derived. Five values were used to derive the regression, excluding data from stations 3 and 6. Using this empirical relationship, a calculated  $[\text{Fe}^{+3}]/[\text{Fe}^{+2}]$  ratio can be derived. The calculated  $[\text{Fe}^{+3}]/[\text{Fe}^{+2}]$  ratios are also plotted in Figure 2. Since the total iron concentrations are different at each station, we use the average value of total iron concentration to represent the original total iron concentration in the seepage. Then using the  $[\text{Fe}^{+3}]/[\text{Fe}^{+2}]$  ratio at each station, the estimated ferrous ion concentrations are calculated. The calculated  $[\text{Fe}^{+2}]$  values are listed in the last column in Table 2.

The iron oxidation process is described both as homogeneous or heterogeneous (Sung and Morgan 1980). The homogeneous process takes place in pure solutions, where the oxidation rate is related to ferrous concentration, water pH and oxygen pressure. The rate law expression is

$$-d[\text{Fe}^{+2}]/dt = k[\text{OH}^-]^2 P(\text{O}_2) [\text{Fe}^{+2}] \quad 3$$

$[\text{Fe}^{+2}]$  is ferrous ion concentration in solution;  $[\text{OH}^-]$  is the concentration of hydroxyl ions;  $P(\text{O}_2)$  is the partial pressure of oxygen in the air. In a buffered solution and under atmospheric pressure, equation 3 can change into

$$-d[\text{Fe}^{+2}]/dt = k_1 [\text{Fe}^{+2}], \quad 4$$

where  $k_1 = k[\text{OH}^-]^2 P(\text{O}_2)$ . Previous laboratory work has shown that  $k$  ranges from  $6 \times 10^{11}$  to  $1.36 \times 10^{14} \text{ M}^{-2} \text{atm}^{-1} \text{min}^{-1}$  (Sung and Morgan 1980).

Although the pH is not constant in the field, the values measured in the ditch resulted in a pseudo first order reaction rate (Figure 3). Using the homogeneous equation to analyze the calculated  $[\text{Fe}^{+2}]$  values, a plot of  $\ln([\text{Fe}^{+2}]/[\text{Fe}^{+2}]_0)$  versus time gives a regression coefficient  $r=0.80$ . The reaction rate constant that is derived has a  $k_1 = 0.0003 \text{ min}^{-1}$ . If we assume  $p(\text{O}_2)=0.2 \text{ atm}$

and consider the average water pH as 5.4, then  $k = 2.38 \times 10^{14} \text{ M}^{-2} \text{atm}^{-1} \text{min}^{-1}$ ; if we assume pH as 6, then  $k = 1.5 \times 10^{13} \text{ M}^{-2} \text{atm}^{-1} \text{min}^{-1}$ . These values are in the range reported by Sung and Morgan (1980) in buffered solutions. This suggests that, under field conditions in AMD seepage, the iron oxidation rate is comparable to that of a buffered system.

The heterogeneous oxidation process refers to a solution that contains ferric hydroxide precipitates. Under these conditions, ferrous oxidation is catalyzed by ferric precipitates.

Here the rate law expression is

$$-d[\text{Fe}^{+2}]/dt = \{k_1 + k_2[\text{Fe}^{+3}]\}[\text{Fe}^{+2}] \quad 5$$

$$\text{and } k_2 = k_s[\text{O}_2]K/[\text{H}^+] \quad 6$$

where  $k_s$  is the surface rate in  $\text{M}^{-1} \text{min}^{-1}$ ,  $[\text{O}_2]$  is the concentration of oxygen in solution, and  $K$  is the adsorption constant of ferrous iron on ferric hydroxide of  $10^{-9.6} \text{ mol/mg}$ .

The conditions requisite for the heterogeneous oxidation process are similar to the conditions found in seepage collection ponds, where large quantities of ferric hydroxide are precipitated. Although the Copper Cliff ditch is also covered by ferric precipitate, the analysis of field data using the heterogeneous oxidation equations 5 and 6 resulted in negative  $k_1$  value, which is unreasonable. It could be that the settled precipitate on the bottom of the ditch has a very low reactive surface area, hence  $k_s$  or  $K$  is too small to allow the heterogeneous oxidation reaction.

Em and pH values of the seepage and tailings pore water used in the laboratory experiments are summarized in Table 4. All pH values decreased with time, and the Em increased with time. The oxidation behavior in the seven water samples varied significantly between samples, as indicated by the data in Figures 4 through 10, where changes in  $[\text{Fe}^{+2}]$  are plotted against reaction time. Data indicate that at least two types of reactions take place in the solutions. One of the reactions is the reduction of ferric to ferrous iron, exemplified by samples 1, 4, and 5. Given that the pH and Em conditions would favor oxidation, the most probable cause for iron reduction is bacterial metabolism. Iron-reducing bacteria are ubiquitously distributed, but require anaerobic conditions for growth. The second reaction is the oxidation of ferrous to ferric iron, as in samples 2, 3, 6, and 7.

The different reaction behaviors might be related to the sampling location, particularly when either ponding or depth of sample collection is considered. All water samples collected from deeper areas initially showed only iron reduction, and then later showed iron oxidation reactions. Sample 2 was aged for more than 1 year, and the oxidation started immediately. However, in sample 1, which was collected at the same location but aged only 1 month, iron was initially reduced. This suggests that as seepage emerged, iron-reducing bacteria in the water continue to metabolize iron for a period of time, even in the presence of air.

Samples 3 and 4 were collected from a uranium seepage pond, at the same location, but one sample was collected from the surface and the other from the bottom of the pond. Both samples had considerably higher iron concentrations than samples 1 and 2, but again their behaviors were different. The bottom water sample showed iron reduction with ferrous increasing during the experiment, whereas, in the surface water, the concentrations of ferrous were relatively constant at the beginning of the experiment. Thus, for about 6,000 minutes a balance existed between oxidizing and reducing reactions. After that time oxidation was the dominant reaction in the solution. Sample 5 was the original seepage that was later ponded (samples 3 and 4). This sample reflected the oxidizing-reducing equilibrium between samples 3 and 4.

A similar behavior is noted for samples 6 and 7. Both are tailings pore water, but collected from different depths in the tailings. Iron in the deep sample took several days to commence oxidation. The shallow sample displayed the oxidation reaction from almost the beginning of the experiment.

For all the experimental data pseudo first order reaction curves were used to simulate the oxidation reactions. The calculations indicated that, with different concentrations of ferrous iron in the AMD seepage and with different initial seepage pH values, the oxidation reaction rate constants were quite similar, ranging from 0.00017 to 0.0003 per minute (Figures 5, 6, 9, and 10). The values were also similar to the field measurements.

Since all the comparable samples were collected from the same locations, the chemical components of those samples were similar. It is a common feature for all the comparable pairs, that in shallow or aged samples oxidation reaction started immediately, while in deep or fresh samples oxidation reactions were out competed or covered by reduction reactions. The probable cause for these different reaction behaviors is microbial metabolism. Laboratory experimental samples were all collected from field ponds or pore water, they are full with suspended solids of ferric. Anaerobic bacteria such as iron-reducers are usually found in greater numbers on pond bottoms and deeper in the tailings. Given the

sample behavior and the probable presence of chemotrophic bacteria, we suspect that the iron reactions noted above are affected by microbial metabolism.

In solution may exists the following equilibrium equation:



Iron oxidation moves  $\text{Fe}^{+2}$  ions into  $\text{Fe}^{+3}$  ions. However, iron reducers may reduce  $\text{Fe}^{+3}$  into  $\text{Fe}^{+2}$  and hence dissolve more  $\text{Fe}^{+3}$  from suspended solids. At the beginning when iron reducing reaction is overwhelmed, ferrous concentration may increase, but ferric concentration is also increased, and the ratio of  $\text{Fe}^{+3}/\text{Fe}^{+2}$  increases. Therefore, in some samples although ferrous concentration increases, Em of the solutions still increase.

## CONCLUSION

The present study of the iron oxidation process in seepages with a pH range of 1.81 to 3.66 and an iron concentration range from 10 mg/L to 4000 mg/L (0.2 mM to 72 mM) suggests that the AMD oxidation process in the open air can be expressed as a pseudo first-order reaction, which varies little over a wide range of AMDs. Oxidation time calculated from this equation can be used to determine

the retention time of AMD seepage precipitation ponds. However, bacterial contribution to the reactions has to be added to the design criteria.



## REFERENCES

- American Public Health Association, 1989. Ferrous iron tested by phynanthroline method. in Standard Methods for the Examination of Water and Wastewater 17th ed. American Water Works Association and Water Pollution Control Federation. p. 3-102.
- Henrot, J. and R. K. Weider, 1990. Processes of iron and manganese retention in laboratory peat microcosms subjected to acid mine drainage. J. Environ. Qual., 19: 312-320.
- Hem, J.D., 1985. Studies and interpretation of the chemical characteristics of natural water. US. Geol. Surv., Water-Supply Paper 2254, 3rd ed. p. 264.
- Hustwit, C. C., T. E. Ackman and P. M. Erickson, 1992. Role of oxygen transfer in acid mine drainage treatment. Report of Investigations, Bureau of Mines, 9405.
- Liu, J. Y. and M. Kalin, 1992. Determination of metal ions in acid mine drainage using a simple titration method. Presentation on the 42nd Annual Canadian Chemical Engineering Conference, Oct. 18-21, 1992.

Nakamura, K., T. Noike and J. Matsumoto, 1986. Effect of operation conditions on biological Fe+2 oxidation with rotating biological contactors. *Wat. Res.* 20(1): 73-77.

Nordstrom, D. K. 1985. The rate of ferrous iron oxidation in a stream receiving acid mine effluent. *US. Geol. Surv., Water-Supply paper* 2270, 113-119.

Okereke, A. and S. E. Jr. Stevens, 1991. Kinetics of iron oxidation by thiobacillus ferrooxidans. *Appl. Environ. Microbio.* 57(4): 1052-1056.

Sung, W. and J. J. Morgan, 1980. Kinetics and product of ferrous iron oxygenation in aqueous systems. *Environ. Sci. Tech.*, 14(5): 561-568.

Wichlacz, P. L. and H. Olem, 1993. Kinetics of biological ferrous iron oxidation. EG and G Idaho, Inc., Idaho Falls. Corp. Source Codes: 046580000; 9507781. Sponsor: Tennessee Valley Authority, Chattanooga.; Department of Energy, Washington, DC. Report No.: Egg-M-27484; CONF-850211-12

Wichlacz, P. L. and F. U. Richard, 1993. A model of ferrous iron oxidation for attached bacteria. Graduate program in Ecology, The PA State Univ.

Table 1. Description of sample sites

Sample	Description	Date
No.1	Base metal seepage collection pond	26/08/93
No.2	Base metal seepage collection pond (stored 1 year in laboratory)	10/08/92
No.3	Uranium seepage collection pond - surface	26/08/93
No.4	Uranium seepage collection pond - bottom	26/08/93
No.5	Uranium seepage - not ponded	26/08/93
No.6	Uranium tailings pore water (70-80cm deep)	26/08/93
No.7	Uranium tailings pore water (20-30cm deep)	26/08/93

**Table 2. Field data for ferrous oxidation measurement**

Station	pH	Fe+2 (mg/L)	Tot. Fe (mg/L)	Ave.Fe+2 (mg/L)	Ave.Fe (mg/L)	[Fe+3]/[Fe+2]	Em (mV)	Length (m)	Cross-section Area(cm2)	Flow Rate (cm3/sec.)	Retention Time (min.)	Fe+2 cal (mg/L)
1A		144.5	178.4									
1B	5.93	154.3	160.4	149.4	169.4	0.134	-62	0.00	112	193	0.0	167.4
2A		127.3	161.9									
2B	5.70	153.1	171.9	140.2	166.9	0.191	-54	8.13	1055	128	111.7	166.5
3A		150.6	159.0									
3B	5.48	165.4	166.2	158.0	162.6	0.029	-32	11.78	745	237	173.4	164.0
4A		128.5	158.3									
4B	5.13	155.5	160.4	142.0	159.4	0.122	14	20.63	135	237	193.0	158.1
5A		155.5	232.2									
5B	4.15	156.8	254.5	156.2	243.4	0.558	188	29.48	1311	237	464.8	125.9
6A		160.5	166.2									
6B	4.11	149.4	178.4	154.9	172.3	0.112	121	32.69	1200	237	740.6	140.1
7A		158.0	263.8									
7B	3.98	151.9	239.4	154.9	251.6	0.624	222	40.85	1602	237	1200.8	117.9

**Table 3. Major Elements in the Field Seepage**

pH	Ca (mg/L)	Fe (mg/L)	K (mg/L)	Mg (mg/L)	Mn (mg/L)	Na (mg/L)	Ni (mg/L)	S (mg/L)	Si (mg/L)
4.39	408	220	70	197	4	110	27	819	20

1994 Liu, J.Y. and M. Kalin, "Study of Ferrous Oxidation Process in AMD Seepage"  
**Table 4. Em and pH changes of AMD oxidation process in laboratory**  
 Proceedings of the International Conference on Environmental Engineering, Pennsylvania, April 24-29, p. 420.

No.1	hour	0.0	2.5	16.5	26.0	39.3	65.3	86.8	120.0	146.0	170.0	191.0	277.0	325.0	454.0
	pH	3.66	3.57	3.51	3.56	3.51	3.48	3.49	3.46	3.47	2.37	3.32	2.98	2.91	2.67
	Em	267	276	276	280	282	283	283	283	282	302	314	372	391	559
No.2	hour	0.0	2.5	14.5	26.3	39.5	65.8	87.4	121.0	146.0	171.0	191.0	277.0	325.0	
	pH	2.45	2.47	2.49	2.50	2.48	2.39	2.38	2.38	2.40	2.37	2.39	2.31	2.34	
	Em	527	534	530	541	549	543	543	535	537	535	534	534	532	
No.3	hour	0.0	2.5	16.3	26.3	39.7	65.9	87.6	121.0	147.0	170.0	191.0	277.0	325.0	454.0
	pH	2.41	2.44	2.50	2.47	2.45	2.40	2.42	2.48	2.46	2.48	2.47	2.37	2.36	2.35
	Em	382	394	392	393	397	398	402	415	400	542	574	571	571	577
No.4	hour	0.0	2.5	15.3	26.7	40.0	66.5	87.8	122.0	147.0	171.0	192.0	278.0	326.0	454.0
	pH	3.24	3.22	3.23	3.20	3.16	3.05	2.99	2.90	2.98	2.78	2.74	2.53	2.42	2.19
	Em	243	252	258	265	270	275	279	281	283	284	286	301	315	350
No.5	hour	0.0	2.5	15.5	26.8	40.3	66.8	88.0	122.0	147.0	171.0	192.0	278.0	326.0	454.0
	pH	1.81	1.87	1.87	1.88	1.86	1.74	1.76	1.74	1.75	1.76	1.77	1.79	1.81	1.89
	Em	356	375	367	368	375	377	374	370	374	376	372	404	435	598
No.6	hour	0.0	2.5	15.8	27.1	40.6	67.1	88.3	122.0	148.0	172.0	192.0	278.0	327.0	454.0
	pH	2.40	2.42	2.47	2.46	2.48	2.46	2.47	2.46	2.48	2.42	2.41	2.29	2.28	2.24
	Em	372	373	375	377	379	384	390	403	404	428	455	618	612	637
No.7	hour	0.0	2.5	16.1	27.3	40.8	67.5	88.5	123.0	148.0	172.0	193.0	279.0	327.0	
	pH	2.61	2.62	2.69	2.68	2.67	2.57	2.52	2.44	2.47	2.39	2.40	2.33	2.31	
	Em	377	372	379	386	393	408	426	524	522	587	589	603	604	

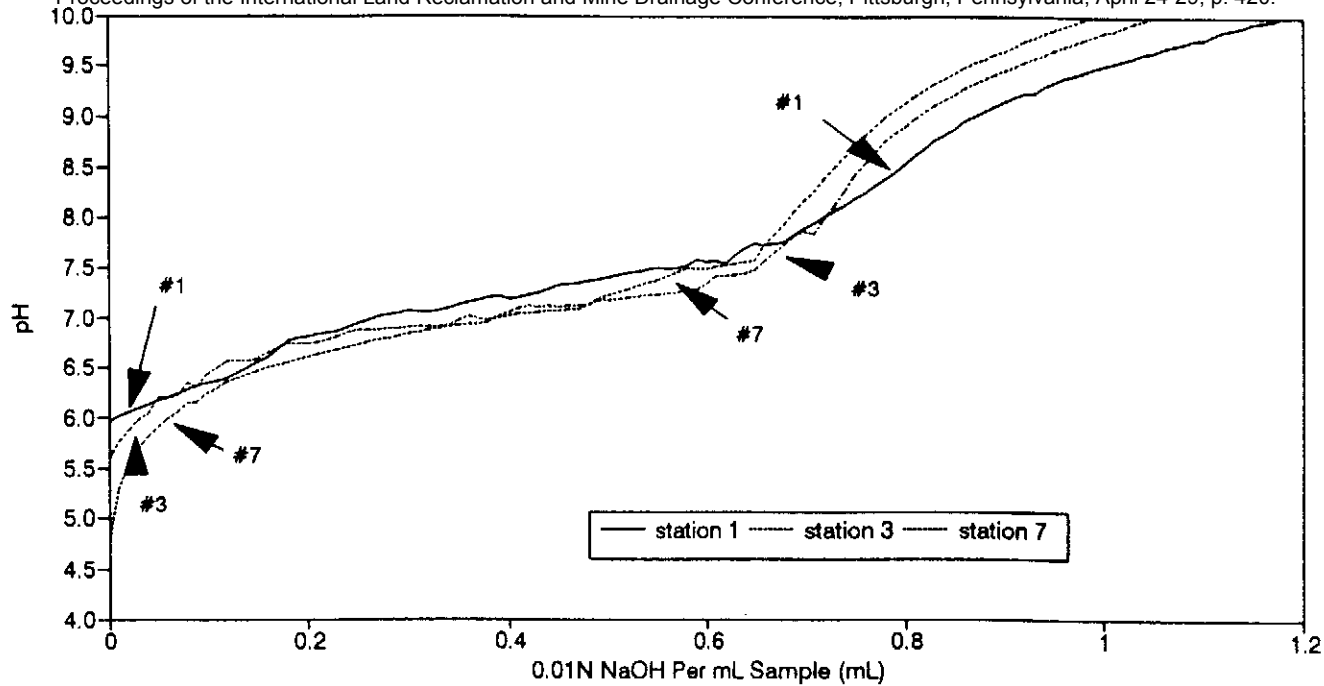


Fig. 1. Field seepage titration curves.

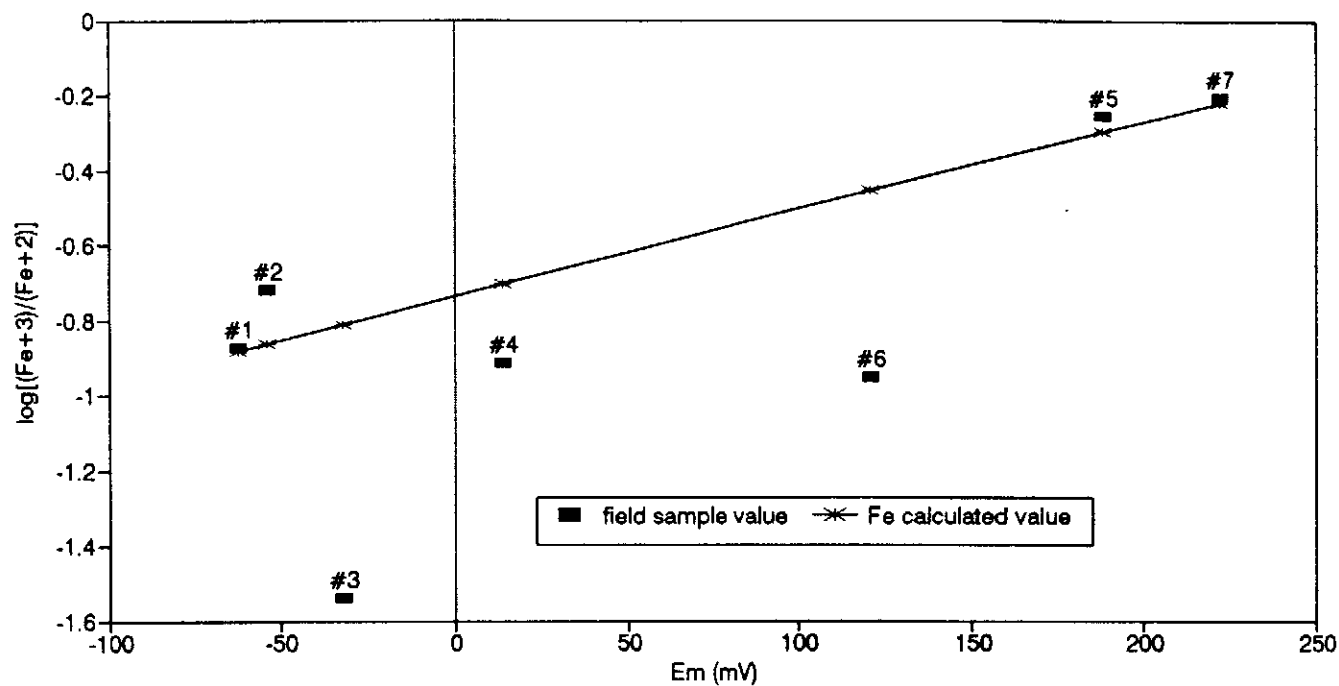


Fig. 2. Calculation of iron concentration and Em.

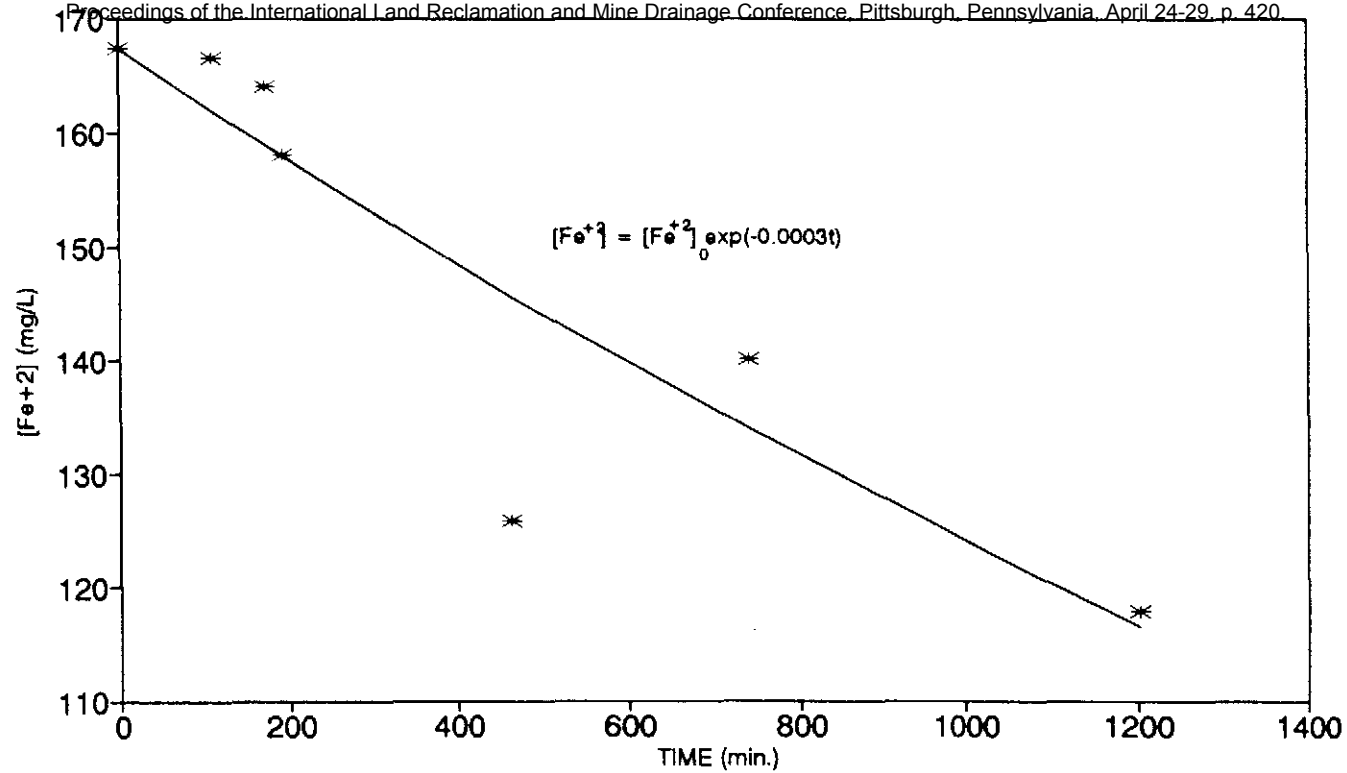


Fig. 3. Field seepage oxidation, homogeneous analysis.

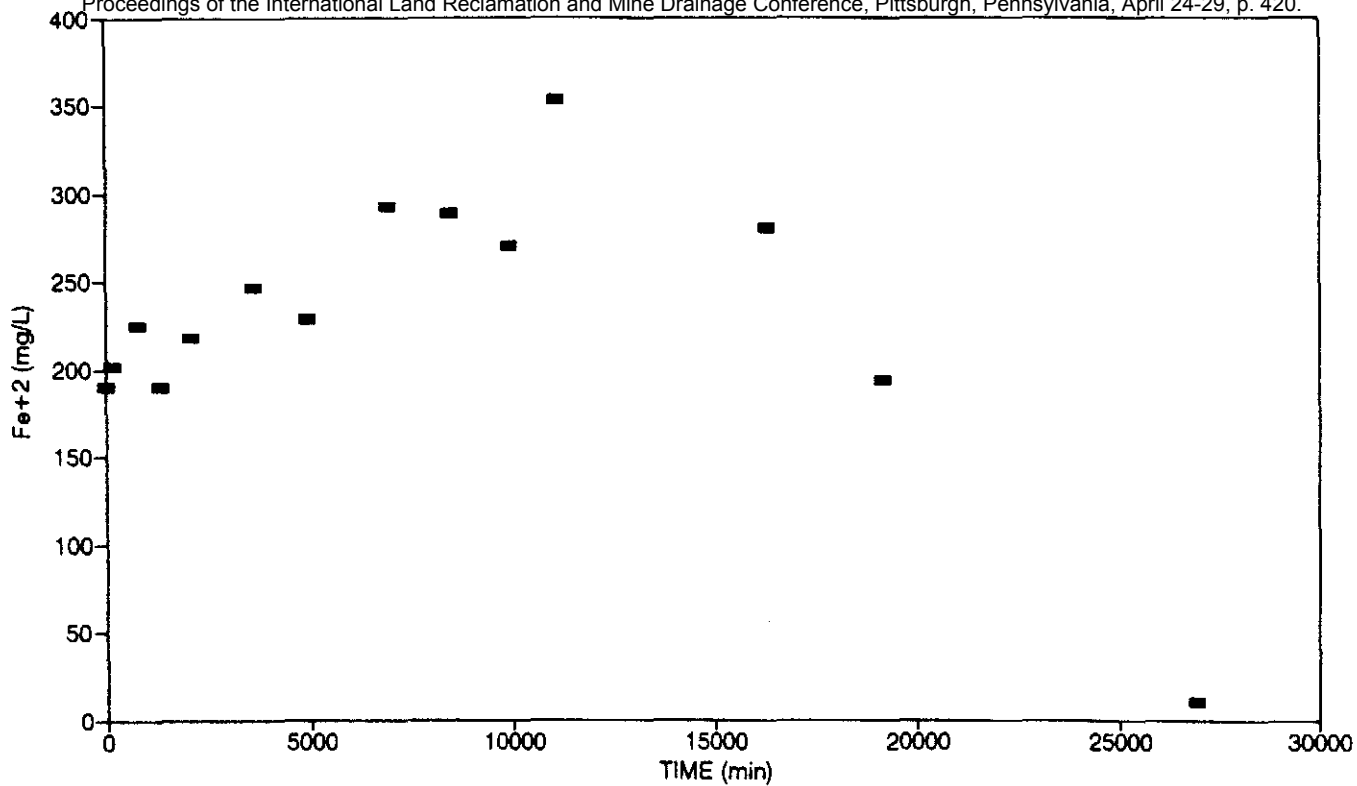


Fig. 4. Sample 1 oxidation.

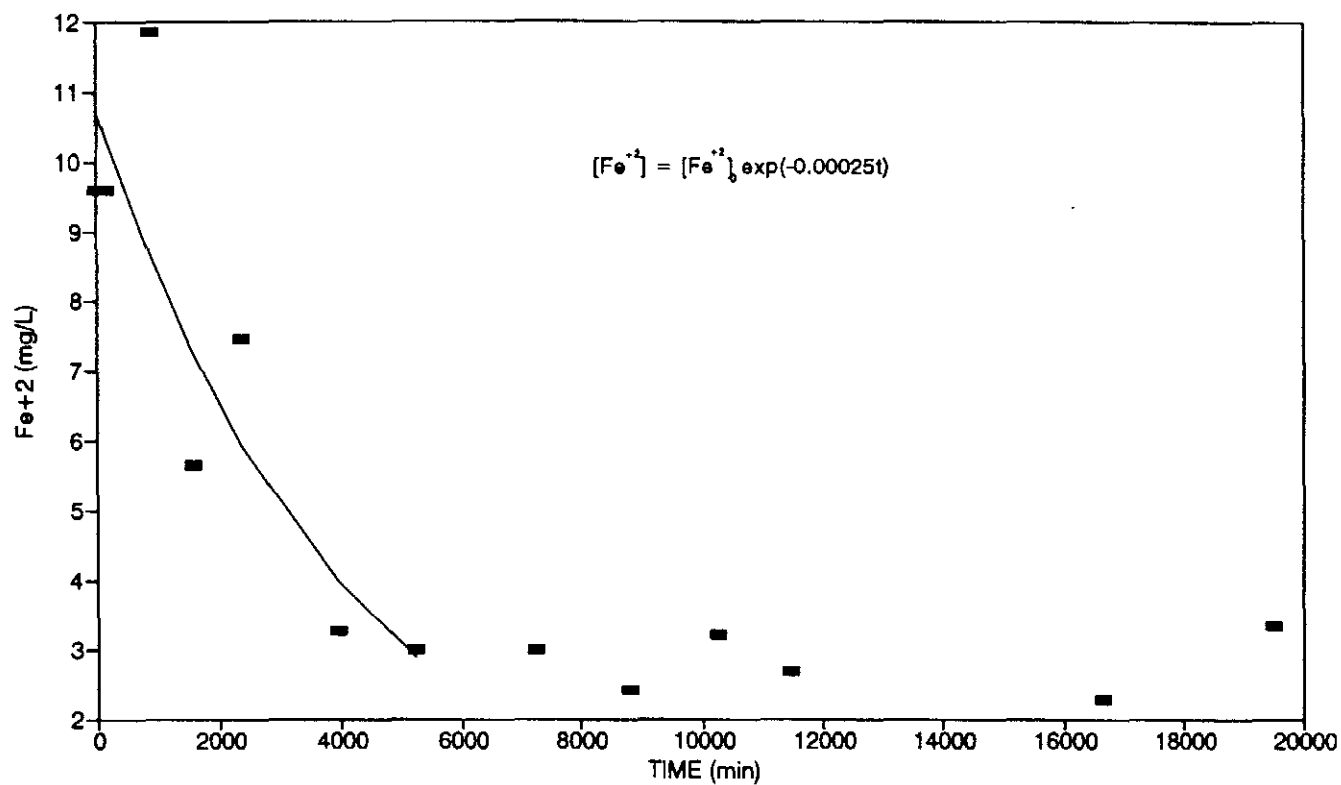


Fig. 5. Sample 2 oxidation.



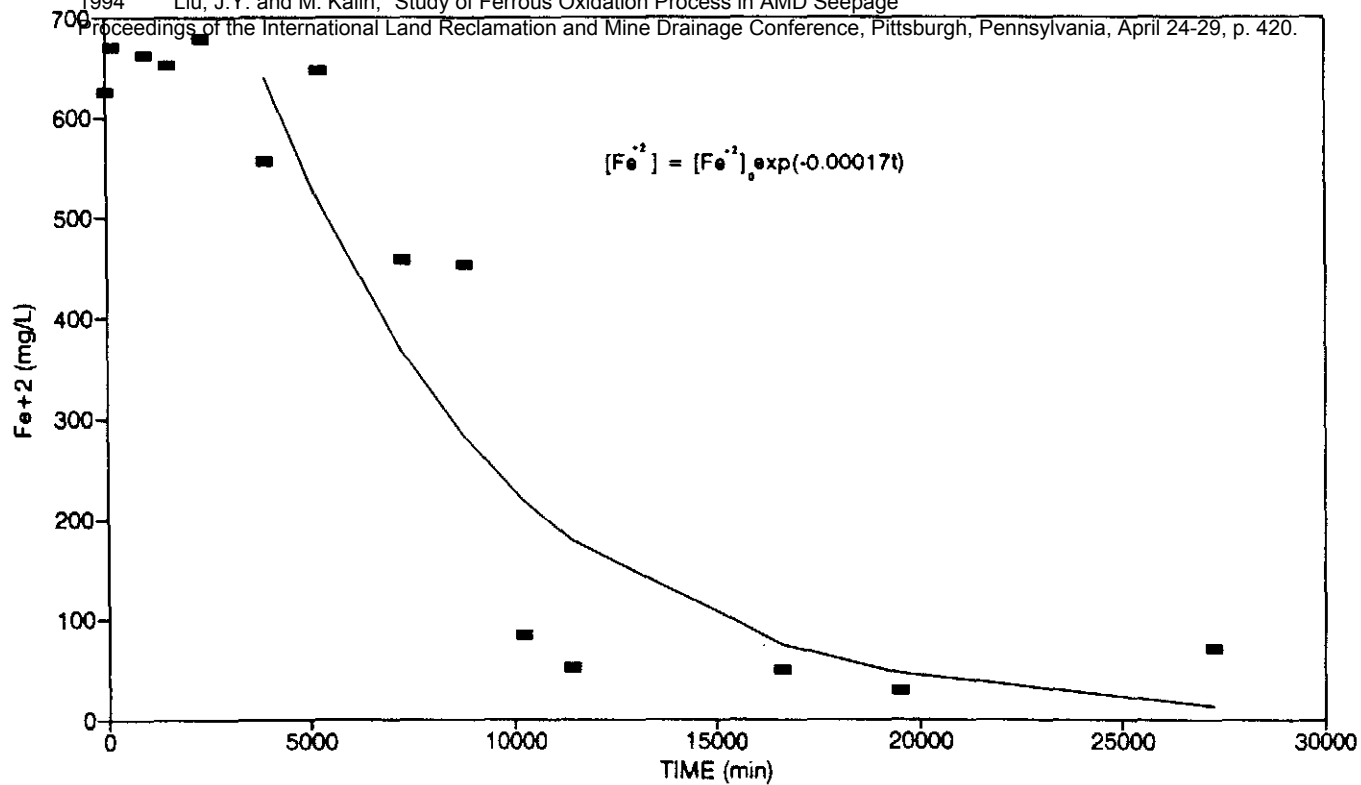


Fig. 6. Sample 3 oxidation.

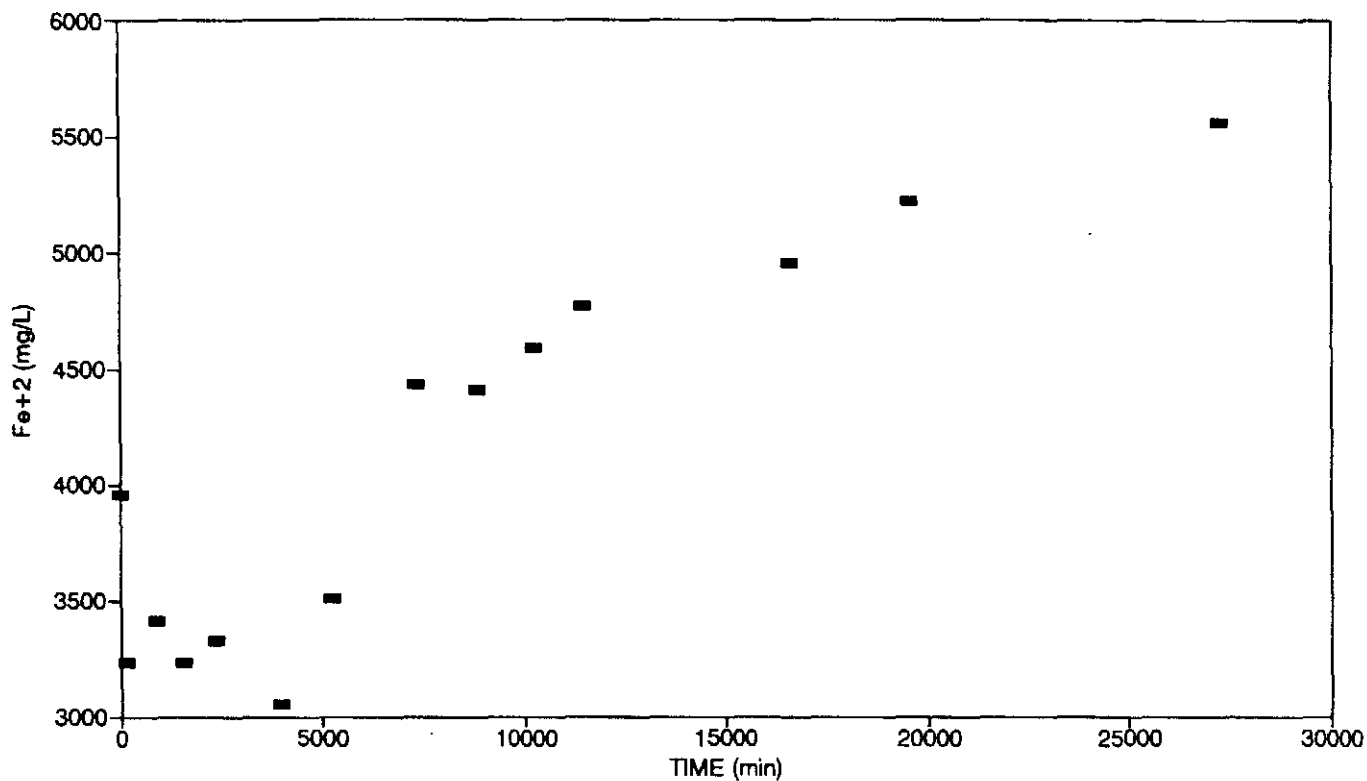


Fig. 7. Sample 4 oxidation.

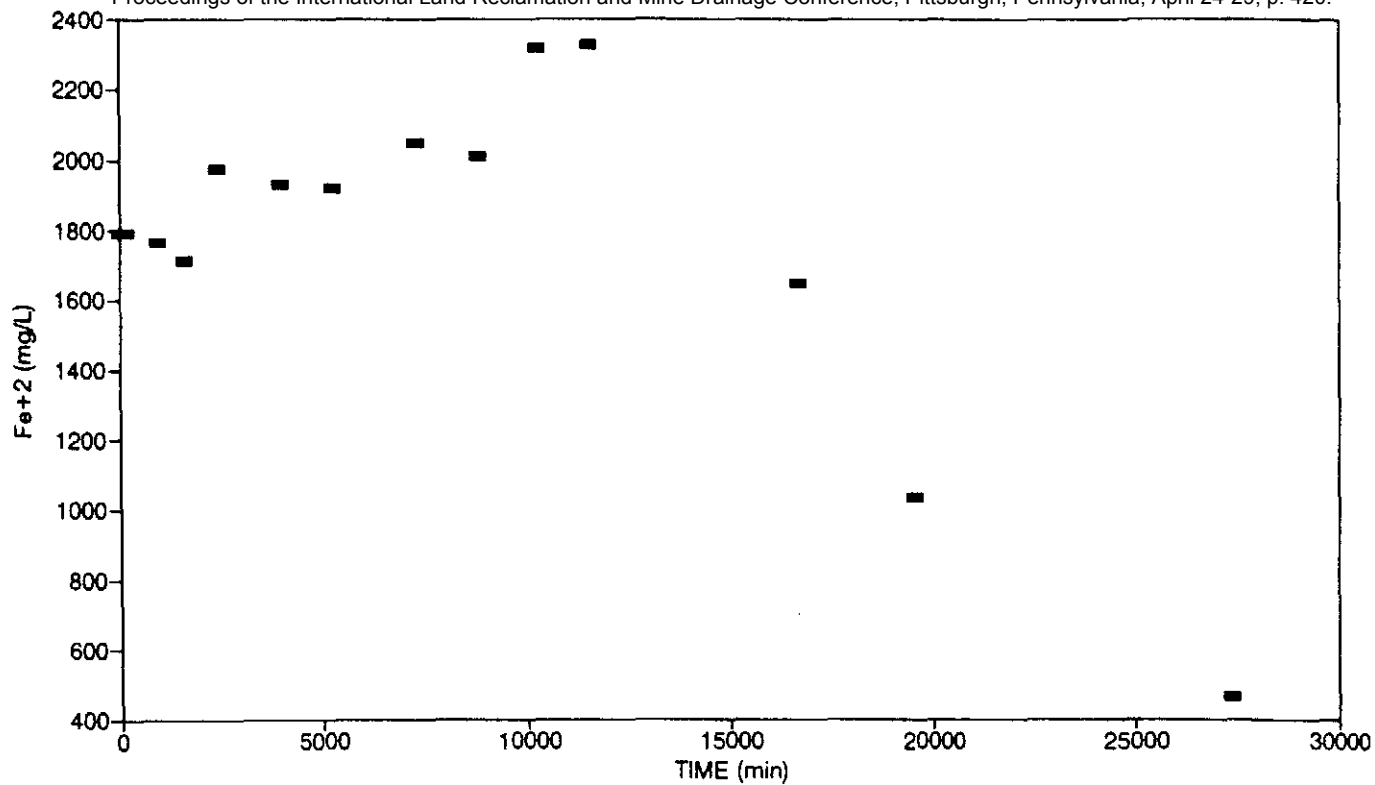


Fig. 8. Sample 5 oxidation.

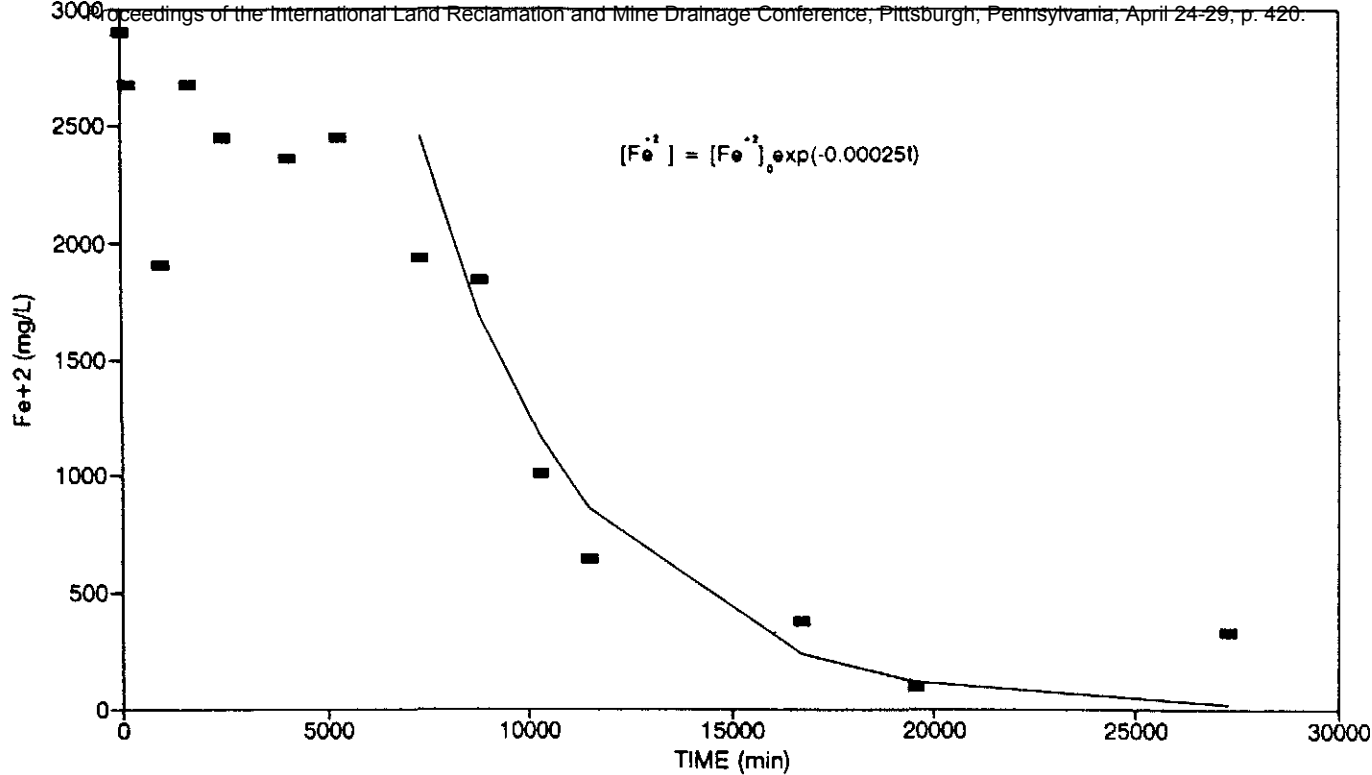


Fig. 9. Sample 6 oxidation.

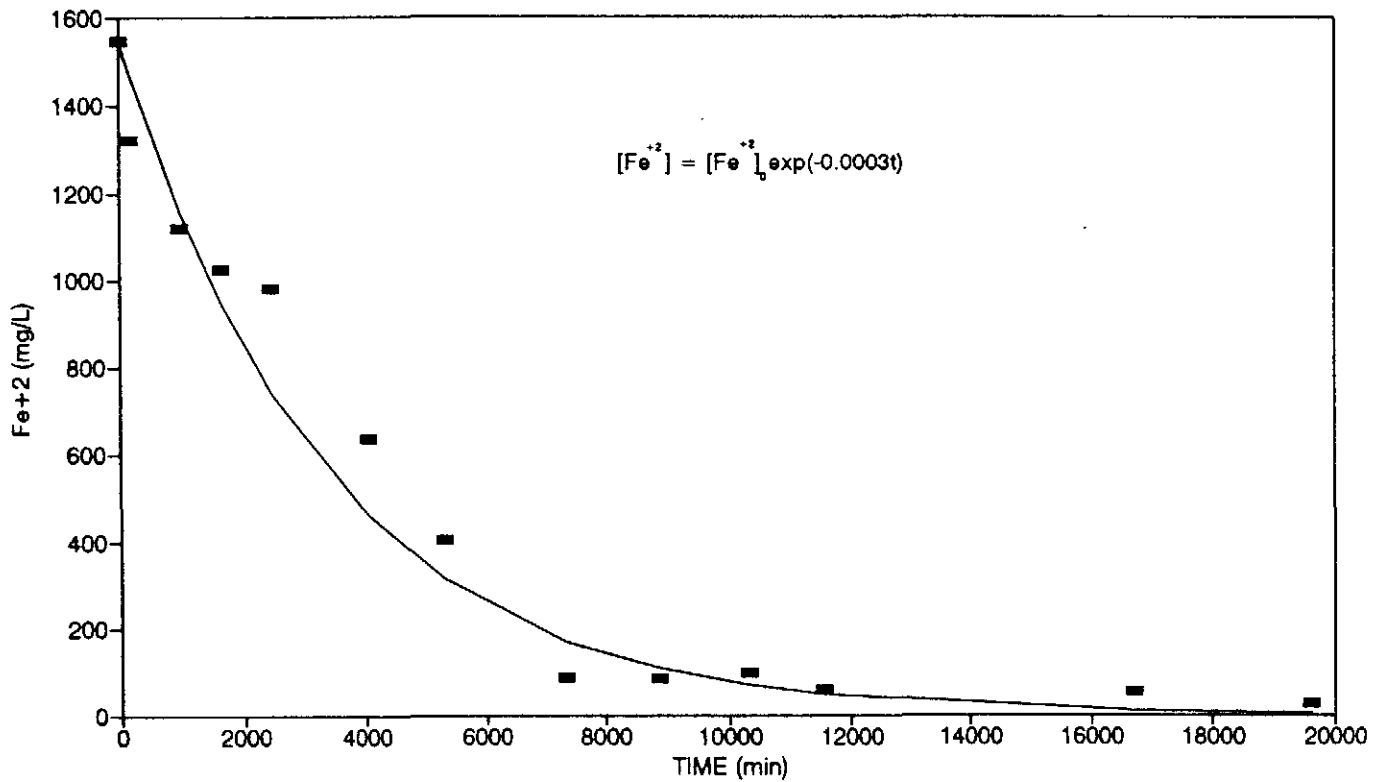


Fig. 10. Sample 7 oxidation.